

New multienzymatic complex formed between human cathepsin D and snake venom phospholipase A₂

Jeane do Nascimento Moraes^{1,2} , Aleff Ferreira Francisco^{3,4,5,6} , Leandro Moreira Dill¹, Rafaela Souza Diniz^{1,2,4,5}, Claudia Siqueira de Oliveira^{1,2}, Tainara Maiane Rodrigues da Silva^{1,7}, Cleópatra Alves da Silva Caldeira^{1,2}, Edailson de Alcântara Corrêa⁸, Antônio Coutinho-Neto¹, Fernando Berton Zanchi^{2,9}, Marcos Roberto de Mattos Fontes³, Andreimar Martins Soares^{4,5,10}, Leonardo de Azevedo Calderon^{1,2,6,11*} 

¹Center for the Study of Biomolecules Applied to Health (CEBio), Oswaldo Cruz Foundation (FIOCRUZ), Porto Velho, RO, Brazil.

²Graduate Program in Experimental Biology (PGBIOEXP), Department of Medicine (DEPMED), Federal University of Rondônia (UNIR), Porto Velho, RO, Brazil.

³Department of Biophysics and Pharmacology, Botucatu Biosciences Institute (IBB), São Paulo State University (UNESP), Botucatu, SP, Brazil.

⁴Laboratory of Biotechnology of Proteins and Bioactive Compounds (LABIOPROT), Oswaldo Cruz Foundation (FIOCRUZ), Porto Velho, RO, Brazil.

⁵National Institute of Science and Technology of Epidemiology of the Western Amazon, INCT-EPIAMO, Porto Velho, RO, Brazil.

⁶Smart Active Ingredients Lab (SAIL), Porto Velho, RO, Brazil.

⁷Faculty of Medicine, University of Buenos Aires (UBA), Buenos Aires, Argentina.

⁸Federal Institute of Education, Science and Technology of Rondonia (IFRO), Porto Velho, RO, Brazil.

⁹Bioinformatics and Medicinal Chemistry Laboratory (LABIOQUIM), Oswaldo Cruz Foundation (FIOCRUZ), Porto Velho, RO, Brazil.

¹⁰São Lucas University Center (UniSL), Porto Velho, RO, Brazil.

¹¹Aparício Carvalho University Center (FIMCA), Porto Velho, RO, Brazil.

Keywords:

Cathepsin D
Phospholipases A₂
Snake venom
Enzyme complex

Abstract

Background: Cathepsin D (CatD) is a lysosomal proteolytic enzyme expressed in almost all tissues and organs. This protease is a multifunctional enzyme responsible for essential biological processes such as cell cycle regulation, differentiation, migration, tissue remodeling, neuronal growth, ovulation, and apoptosis. The overexpression and hypersecretion of CatD have been correlated with cancer aggressiveness and tumor progression, stimulating cancer cell proliferation, fibroblast growth, and angiogenesis. In addition, some studies report its participation in neurodegenerative diseases and inflammatory processes. In this regard, the search for new inhibitors from natural products could be an alternative against the harmful effects of this enzyme.

Methods: An investigation was carried out to analyze CatD interaction with snake venom toxins in an attempt to find inhibitory molecules. Interestingly, human CatD shows the ability to bind strongly to snake venom phospholipases A₂ (svPLA₂), forming a stable multi-enzymatic complex that maintains the catalytic activity of both CatD and PLA₂. In addition, this complex remains active even under exposure to the specific

* **Correspondence:** calderon@unir.br

<https://doi.org/10.1590/1678-9199-JVATITD-2022-0002>

Received: 13 January 2022; Accepted: 16 August 2022; Published online: 04 November 2022



inhibitor pepstatin A. Furthermore, the complex formation between CatD and svPLA₂ was evidenced by surface plasmon resonance (SPR), two-dimensional electrophoresis, enzymatic assays, and extensive molecular docking and dynamics techniques.

Conclusion: The present study suggests the versatility of human CatD and svPLA₂, showing that these enzymes can form a fully functional new enzymatic complex.

Background

Cathepsins compose a family of lysosomal proteases mainly found in acidic endo/lysosomal compartments and are implicated in a broad spectrum of physiologic processes, such as intracellular protein degradation, energy metabolism, hormonal regulation, bone resorption, and immune responses [1]. These proteins belong to three protease families, characterized based on differences in the following amino acids at their active site: aspartic proteases (D and E), serine proteases (A and G), or cysteine proteases (B, C, H, F, K, L, O, S, V, X, and W) [1–4].

Furthermore, cathepsins are essential to maintaining cell homeostasis [5]. The inactivation, loss of function, and overexpression of these proteases can result in inappropriate degradation and abnormal accumulation of lysosomal waste [1, 6]. In addition, extracellular oversecretion of cathepsins is associated with uncontrolled cell proliferation, invasion, and differentiation, which in turn may bring about the onset of fatal pathologies, including atherosclerosis, cancer, and tissue fibrosis [6–12].

Due to its physio-pathological functions, cathepsin D (CatD) is one of the most studied lysosomal proteases [13–15]. CatD is an aspartic endopeptidase with two conserved Asp residues in its active site; these residues tend to deprotonate, indicating that the pH-optimum of activity resides at pH values below 5 [16]. In addition, CatD has three distinct regions that are characteristic of aspartic proteases, an N-terminal domain (residues 1–188), a C-terminal domain (residues 189–346), and an interdomain, antiparallel/3-sheet formed by the N-terminus (residues 1–7), the C-terminus (residues 330–346), as well as the linker residues between domains (160–200) [17].

Considered a multifunctional enzyme due to its involvement in various biological processes, CatD operates in both cytosolic and extracellular environments [13, 18–22]. Studies have shown that CatD is involved in the activation of precursors of biologically active proteins in pre-lysosomal compartments of specialized cells [11, 20, 23]. This enzyme is indispensable for cellular functions such as cell migration, differentiation, growth, cycle progression, tissue remodeling, and neovascularization activation [6, 11, 12, 19, 22, 24–27]. Additionally, CatD is involved in initiating the apoptotic cascade [28, 29] in lysosomal cell death pathways [22, 25].

CatD is directly related to the pathogenesis and progression of degenerative diseases [6, 30], such as lymphoid cell degeneration [31], Parkinson's [32] and Alzheimer's disease [33], atherosclerosis [34], and different types of cancer [35, 36]. For instance, some cell types under pathological conditions overexpress and secrete

CatD to the extracellular environment via lysosomal release [20]; this makes CatD an important tumor marker in breast, bladder, and mouth cancers, among others [35, 36]. Furthermore, due to the participation of cathepsins in a broad spectrum of diseases, these proteases are promising therapeutic targets for small molecules and peptide drugs [33, 36].

In order to investigate human CatD inhibitors for the design and development of tools and agents of scientific and therapeutic interest, snake venoms belonging to the genera *Bothrops*, *Crotalus*, and *Lachesis* have been used as natural sources of biologically active molecules able to act selectively and specifically on different cellular targets [37, 38]. Of all the bioactive molecules present in snake venoms, phospholipases A₂ (svPLA₂) are among the most frequently encountered and studied [39, 40]; these proteins have established physical-chemical properties and a variety of pharmacologic and toxic effects in snakebite envenomation, such as myonecrosis, anticoagulation, platelet aggregation inhibition, neurotoxicity, cardiotoxicity, hypotension and edema formation [41–45].

Interestingly, human CatD shows the ability to bind strongly to svPLA₂s, forming a stable and functional complex that is able to remain active even at pH values higher than 5 and is also unaffected by the inhibitor pepstatin A. These results, presented and discussed below, demonstrate the multifunctionality and versatility of CatD, warranting many new possibilities for the understanding of cathepsin functions in cytosolic and extracellular environments during physiologic and pathologic processes. Therefore, the present study aims to demonstrate and characterize an enzymatic complex formed by human CatD and a snake venom phospholipase A₂.

Methods

Cathepsin D

Cathepsin D (cod. C8696) was obtained from Sigma-Aldrich Ltda and prepared according to the manufacturer's recommendations.

Snake venoms

All snake venoms used in this study were acquired from the Venom Bank at CEBio/Fiocruz Rondônia/UNIR (Centro de Estudos de Biomoléculas Aplicadas a Saúde), Porto Velho, RO, under local government authorization license number: IBAMA nº 27131-3 and CGEN/CNPq 010627/2011-1.

Phospholipases A₂ (PLA₂s)

The Bothropstoxin-I (BthTX-I) and Bothropstoxin-II (BthTX-II) from *Bothrops jararacussu* were obtained from the Venom Bank at CEBio (Centro de Estudos de Biomoléculas Aplicadas a Saúde/Fiocruz Rondônia/UNIR), located in Porto Velho, RO. PLA₂ LmtTX from *Lachesis muta* provided by Diniz-Sousa et al. [46], PLA₂ BnuTX-I from *Bothrops urutu* provided by Corrêa et al. [47], PLA₂ Braziliase-I and Braziliase-II from *Bothrops brazili* provided by Kayano et al. [48] and Sobrinho et al. [49].

Bothrops jararaca snake venom fractionation

B. jararaca venom was solubilized in 50mM ammonium bicarbonate buffer (AMBIC), pH 8.0 and applied to an anion exchange column (CM-Sepharose 10 x 30 cm). The fractions were eluted in a linear gradient of 500 mM AMBIC, pH 8.0 under a flow of 1 mL/min. Absorbances were measured at 215 and 280 nm. The fractions were subjected to salt removal in a 15mL filter (AMICON ULTRA-15) with a 50 kDa cutoff.

Binding assays

Surface plasmon resonance (SPR) molecular interaction assays were performed in a Biacore T200 system (GE Healthcare). Cathepsin D immobilization was done using a CM5 S-type sensor chip via amine coupling. The contact time of each cycle was set at 60 seconds, with a flow rate of 30 µL/min, followed by 60 seconds of dissociation time. For the regeneration stage at the end of each cycle, a 0.5% TFA solution was used with 30 seconds of contact time at a flow of 30 µL/min. All experiments were performed at 25 °C, and binding assays were conducted in phosphate-saline buffer (PBS), pH 7.4 and analytes at a concentration of 100 µg/mL.

Protein quantification

The protein concentrations present in venom samples were determined using Bradford's method [50]. For spectrophotometric measurements, the sample was aliquoted in a 1 mL disposable plastic cuvette along with 1:10 (v/v) Bradford reagent, which was incubated for 15 minutes. Absorbance was monitored at 595 nm using a Biomate 3 spectrophotometer. The calibration curve was performed using bovine albumin (Sigma).

SDS-PAGE

The relative mass of proteins was determined by SDS-PAGE using discontinuous gels, with a stacking gel (4% acrylamide in 0.5 M Tris-HCl buffer, pH 6.8) (Sigma Aldrich, USA) and a resolving gel (12.5% acrylamide in 1.5 M Tris-HCl buffer, pH 8.8). The experimental buffer solution used to fill the wells was 0.06 M Tris-Base, 0.5 M Glycine, and 10% SDS (Sigma Aldrich, USA). The samples with 1M DTT were preheated to 95 °C for 5 min and applied to the stacking gel wells along with the Molecular Weight standard (7 to 175 kDa - BioLabs P7709S, USA). In the electrophoretic run, a current of 15 mA per gel and free

voltage was fixed for 1 hour and 40 minutes. After this, the gel was washed for 15 minutes with a fixing solution (ethyl alcohol 50% and acetic acid 12%) and then stained with Coomassie G-250 blue solution (Sigma Aldrich, USA) for 10-30 minutes. After this period, the gel was bleached in a bleaching solution (20% ethyl alcohol and 3% acetic acid). The gels' images were scanned using Image Scanner III (GE Lifescience Health Care).

The 2D electrophoresis consisted of two steps: isoelectric focusing and 1D SDS-PAGE. For the first dimension, the sample was prepared in a rehydration solution (8 M urea, 2% CHAPS, 0.5/2% IPG buffer, 0.002% bromophenol blue, and 1 M DTT); this same solution was then incubated with a 7-cm strip (pH 3-10, linear) for 12-20 h. After rehydration, the strip was applied to an Ettan IPGphor 3 (GE Healthcare) isoelectric focusing system and later stored at - 80 °C. For the second dimension, the strip was washed with DTT and iodoacetamide diluted in 5 mL of equilibration buffer solution (6 M urea, 2% SDS, 30% glycerol, 50 mM Tris- HCl, pH 7.4, 0.002% bromophenol blue). Then, the strip was applied to a 15% polyacrylamide gel. The gel was stained with Coomassie Blue G-250 and scanned in a GE Image Scanner III apparatus.

Metalloprotease contamination analysis of BthTX-II

Proteolytic activity was evaluated according to the method described by Rodrigues and coworkers [51], with adaptations, using casein as a substrate. Samples (12 µg/mL) were incubated with 250 µL of 2% casein in 0.1 M sodium citrate (pH 3, 4, 5, 6, 7) for 30 minutes at 37 °C, interrupted by the addition of 250 µL of 20% trichloroacetic acid (TCA). Similarly, sample contamination by metalloprotease at different pHs was analyzed by adding 10µL of ethylenediaminetetraacetic acid (EDTA). The solution was left to rest for 30 minutes at room temperature and then centrifuged at 10,000 x g for 15 minutes at 25 °C. The proteolytic activity was estimated based on the absorbance of the supernatant at 280 nm, with trypsin as a positive control.

Proteolytic activity on casein

The proteolytic activity was evaluated according to the method described by Rodrigues et al. [51], with adaptations, using casein as a substrate. Samples (6.3 µg/mL) were incubated with 250 µL of 2% casein in 0.1 M sodium citrate (pH 3, 4, 5, 6, 7) for 30 minutes at 37 °C and then interrupted by the addition of 250 µL of 20% trichloroacetic acid (TCA). The solution was left to stand for 30 minutes at room temperature and then centrifuged at 10,000 x g for 15 minutes at 25 °C. Proteolytic activity was estimated based on the absorbance of the supernatant at 280 nm. The proteolytic activity monitored in SDS-PAGE electrophoresis was performed according to the protocol described above. Inhibition was carried out by means of exposure to high temperatures (90 °C).

Phospholipasic activity on 4N3OBA

This procedure was carried out as described by Petrovic and coworkers [52]. 5 mg of the substrate 4-nitro-3-octanoyloxy-

benzoic acid (4N3OBA) (Enzo Lifescience, USA) was diluted in 5.4 mL of acetonitrile. 0.2 mL aliquots were dried and stored at -20°C . Each tube containing 4N3OBA was diluted in 2 mL of sample buffer (0.01 M Tris-HCl at pH 8.0, 0.01 M CaCl_2 , and 0.1 M NaCl) (Sigma Aldrich, USA) and maintained on ice. In order to determine the phospholipase activity, a total of 190 μL of 4N3OBA reagent combined with 10 μL of sample (cathepsin + BthTX-II, and inhibitor) was applied in a 1:1 ratio, pre-diluted in water and incubated at 37°C ; subsequently, the substrate was added to the samples and immediately incubated at 37°C . The absorbance was measured at 425 nm for 30 minutes (interval of 1 min). Phospholipase activity was considered directly proportional to the increase in absorbance values and expressed as the mean \pm standard deviation; the results were submitted to analysis of variance (ANOVA) followed by Tukey's post-test for $p < 0.05$.

In silico molecular interactions

All PLA₂s used in the *in vitro* assays were assessed through molecular docking against cathepsin D (CatD). The available structures of CatD (4OD9), BthTX-I (3CXI), BthTX-II (2OQD), and Crotoxin B (3R0L) were extracted from the RCSB Protein Data Bank. The structures of Braziliase II (UniProtKB: P0DUN4) and LmutTX (UniProtKB: P0DUN7) were generated by means of comparative modeling using the Rosetta web server [53]. The structural conformation guiding the interaction and complexation of CatD and PLA₂ were predicted through a consensus of 5 protein/protein docking tools (pyDock, ZDOCK, HDock, ClusPro, and GRAMX). The CatD + BthTX-II complex was subjected to molecular dynamics, with five replicas of 100 ns using GROMACS 2020.2 employing the CHARMM36-mar2019 force field [54]. All simulations were carried out with a neutral net charge box of 4 Å radius from the farthest atom, solvated

with TIP3P water, and equilibrated with 100 mM NaCl. The system was minimized with the steepest descent minimization until it reaches the power levels below 100 kJ/mol/nm.

Then, the box was equilibrated under an isochoric-isothermal (NVT) ensemble for 1 ns, generating speeds according to the distribution of Maxwell-Boltzmann at 310.15 K using the V-Rescale thermostat [55] followed by an isothermal-isobaric (NPT) ensemble using the Berendsen barostat at 1 bar [56]. Subsequently, five replicas of unrestrained 100 ns simulations were executed using the Nose-Hoover Thermostat [57] and Parrinello-Rahman barostat [58].

Nonbonded interactions were calculated within a radius of 12 Å using a switching function between 10 and 12 Å. Afterwards, the trajectories were analyzed, and radius of gyration and backbone RMSD measurements were extracted from the main interacting parties for stability assessment. Further, the trajectories were subjected to clusterization using the gromos method [59] with an RMSD distribution of 2 Å. All images and interaction maps were created using UCSF Chimera 1.13.1 [60].

Results

Snake venom binding assays

Snake venoms were screened as to their potential interactions with human CatD, aiming to generate an extensive analysis of binding responses featuring the unique molecular content found in each venom. In this fashion, the bioactive compounds with the most affinity towards CatD could be inferred based on venom composition. For this purpose, thirteen venoms from different species were used (Fig. 1 and Table 1). Among these species, *Bothrops brazili*, *B. jararaca*, *B. jararacussu*, and *B. leucurus* stood out as promising due to their association and dissociation profiles and the maximum number of responses reached.

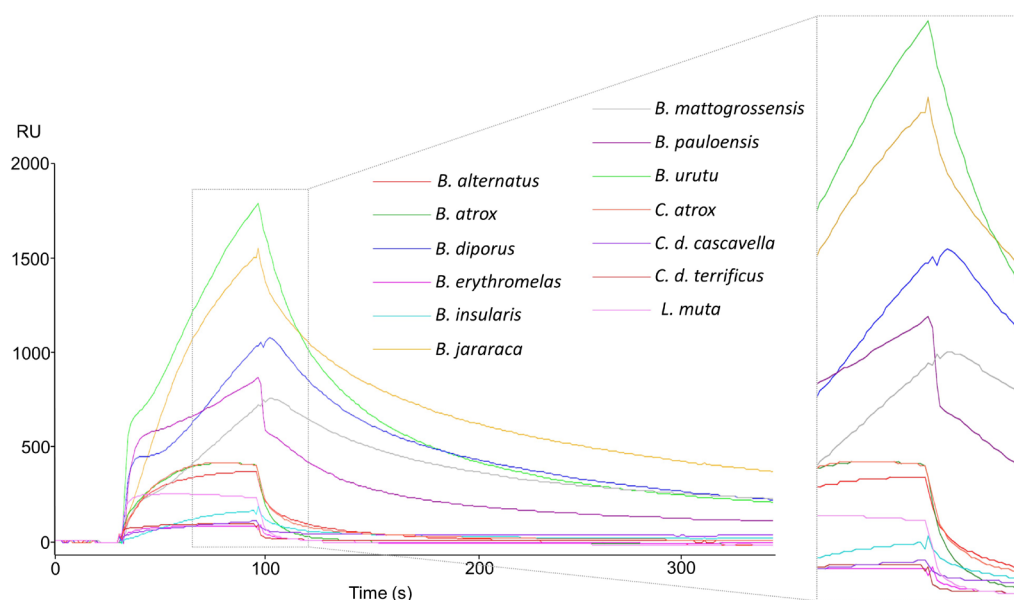


Figure 1. SPR assays between snake venoms and human cathepsin D (CatD). Sensorgrams were generated in a screening round of snake venoms against CatD. All interactions are plotted according to the response upon binding in RU (resonance units).

Bothrops jararaca venom is one of the most well-characterized and studied venoms and showed a significant binding response (1,625 RU mg/mL) with CatD; for those reasons, it was selected for further analysis. In order to identify the venom components

responsible for the majority of interaction signals, *B. jararaca* crude venom was fractionated through cation exchange chromatography (Fig. 2A). The chromatography resulted in 12 fractions that were later submitted to SPR assays against CatD.

Table 1. SPR binding assay of immobilized human cathepsin D with crude snake venoms.

Species	Protein concentration (mg/mL) ^a	Response (RU) ^b	RU/mg
<i>Bothrops alternatus</i>	1.096	342.0	312.0
<i>B. atrox</i>	0.954	378.6	396.9
<i>B. brazili</i>	1.023	1,549	1,514.2
<i>B. diporus</i>	1.051	973.8	927.0
<i>B. erythromelas</i>	1.147	76.5	66.7
<i>B. insularis</i>	0.544	134.0	246.0
<i>B. jararaca</i>	0.867	1,409.3	1,625.5
<i>B. jararacussu</i>	0.887	2,003.1	2,258.3
<i>B. leucurus</i>	0.965	1,508.0	1,562.7
<i>B. mattogrossensis</i>	1.122	665.6	593.2
<i>B. pauloensis</i>	0.734	804.3	1,095.8
<i>B. urutu</i>	1.457	1,663.3	1,141.6
<i>Crotalus atrox</i>	1.470	185.0	125.9
<i>C. d. cascavella</i>	2.934	100.0	34.1
<i>C.d. terrificus</i>	0.779	65.0	83.4
<i>Lachesis muta</i>	1.689	216.7	128.3

^aProtein quantification using the Bradford Method. ^bResponse: maximum response values are presented in resonance unit (RU).

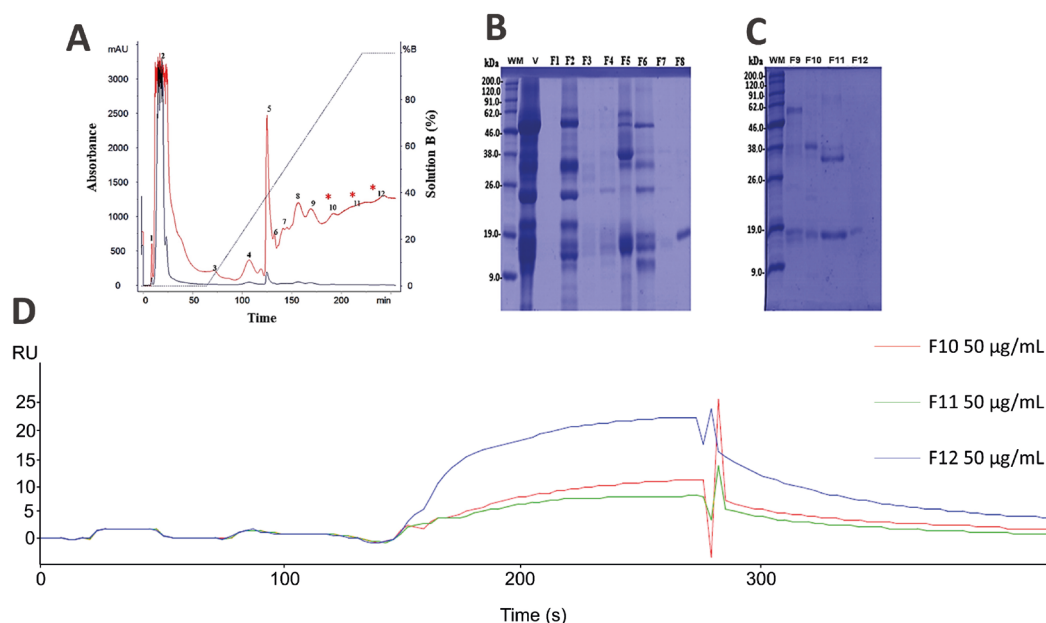


Figure 2. Chromatographic profile of *B. jararaca* snake venom, SDS-PAGE, and binding assays of the isolated fractions. **(A)** The chromatographic profile demonstrates fractionation on a CM-Sepharose column previously equilibrated with 50 mM AMBIC, pH 8.0, and fractions eluted with a 0-100% gradient of 500 mM AMBIC, pH 8.0, at a constant flow rate of 1 mL/min, monitored at 215 (red) and 280 nm (blue). The twelve fractions collected were numbered from 1 to 12, the fractions of interest 10, 11, and 12 being indicated with asterisks (*). **(B)** SDS-PAGE of the 12 fractions from *B. jararaca* venom. **(C)** MM: molecular mass, V: crude venom, and eight fractions named F1 to F8. **(D)** MM: molecular mass, and fractions from F9 to F12. **(D)** Fraction interaction responses: 10 (blue), 11 (green) and 12 (red) with responses of 125, 10 and 12 RUs, respectively.

The subsequent assays revealed that only fractions 10, 11, and 12 presented significant interactions with CatD, showing responses from 25, 12, and 10 RUs at a concentration of 50 mM (Fig. 2D). Next, the protein profile of each fraction was determined by SDS-PAGE, resulting in clear monophoretic bands around 13 kDa for all three fractions (Fig. 2C), compatible with svPLA₂ mass and bands between 30 to 40 kDa, suggesting snake venom metalloproteases (SVMPs) in the fractions 10 and 11 (Fig. 2C). When these fractions were tested for their phospholipase activity, fractions 3, 8, 10, 11, and 12 showed relevant activity against the substrate 4N3OBA (results not shown), confirming the presence of phospholipases in the fractions of interest.

These data strongly suggested that human CatD has the ability to interact with svPLA₂s. In order to investigate this tendency and evaluate the specific affinity between both proteins, six svPLA₂s from the genera *Bothrops* and *Lachesis* were submitted to SPR assays at concentrations of 15 and 50 mM (Table 2).

The binding analysis via SPR spectroscopy revealed that the toxins tested (except BthTX-I and Braziliase I) displayed tight binding to immobilized CatD (Fig. 3). For instance, BthTX-II (an enzymatic Asp-49-PLA₂) [61] presented interaction showing

dose-dependent SPR responses ranging from 420 to 1,420 at concentrations of 15 and 50 mM, respectively (Fig. 3C).

Different from Braziliase-I, Braziliase-II showed a dose-dependent sensorgram of 245 RUs (15 mM) and 837 RUs (50 mM) with a prolonged dissociation phase suggesting a possible low dissociation rate constant (K_d) (Fig. 3A), which could be investigated through further analysis. Both BnuTX-I from *B. urutu* and LmutTX from *L. muta* also interacted with immobilized CatD (Fig. 3B), showing sensorgrams with different intensities of 552 and 2,180 RU at 50 mM [46, 47]. In any case, both showed a similar shape in their association and dissociation curves.

Despite the high level of homology among svPLA₂s, the binding analysis between CatD and these toxins exhibited interactions with different intensity profiles. Nevertheless, the binding profile of CatD towards svPLA₂ displayed high similarity, suggesting a common recognition site. It is worth pointing out that overall, svPLA₂s present a characteristic and consistent tridimensional structure, which could be the driving factor behind the ability of CatD to interact with the svPLA₂s tested in this study [61, 62].

Table 2. SPR interaction assays of immobilized human cathepsin D with svPLA₂s from *Bothrops* and *Lachesis* snake species.

svPLA ₂	Type	Species	Concentration (mM)	Response (RU)
BthTX-I	Lys-49	<i>B. jararacussu</i>	50/15	NC
BthTX-II	Asp-49	<i>B. jararacussu</i>	50/15	1,420/420
Braziliase-I	Asp-49	<i>B. brazili</i>	50/15	NC
Braziliase-II	Asp-49	<i>B. brazili</i>	50/15	837/245
BnuTX-I	Lys-49	<i>B. urutu</i>	50	552
LmutTX	Asp-49	<i>L. muta</i>	50	2,180

Samples that showed distorted results were considered inconclusive (NC).

Enzymatic activity of the cathepsin D + BthTX-II complex

Initially, the apparent molecular mass and isoelectric point (pI) of the CatD + BthTX-II complex, as well as that of both enzymes separately, BthTX-II and CatD, were verified through two-dimensional electrophoresis (Fig. 4), determining a molecular mass of approximately 60 kDa and pI of 5.79 for the CatD + BthTX-II complex. Next, the proteolytic activity of CatD and of its complex with svPLA₂ (BthTX-II) were evaluated using casein as a substrate at pH values of 3, 4, 5, 6, and 7, and Pepstatin A as a specific inhibitor. The optimal enzymatic activity of CatD was observed at pH 5, which is in agreement with previous studies [63]. On the other hand, the CatD + BthTX-II complex proved to be functional at different pH values reaching maximum

activity at pH 6 (Fig. 5), revealing that the binding between these two proteins changes CatD's functionalities, increasing its pH-dependent activity to higher values. Additionally, the CatD + BthTX-II complex is resistant to the inhibitor Pepstatin A at pH 6, suggesting the possibility of changes in enzyme specificity (Fig. 6A).

Similar outcomes were observed in the SDS-PAGE assay, revealing that the bands formed after casein hydrolysis by CatD and CatD + BthTX-II are slightly different (Fig. 6B), suggesting potential differences in cleavage sites and further confirming the *in vitro* enzymatic activity. Furthermore, to rule out any residual contamination from the BthTX-II sample due to venom proteases, this sample was also submitted to the same conditions, and showed no proteolytic activity (results not shown).

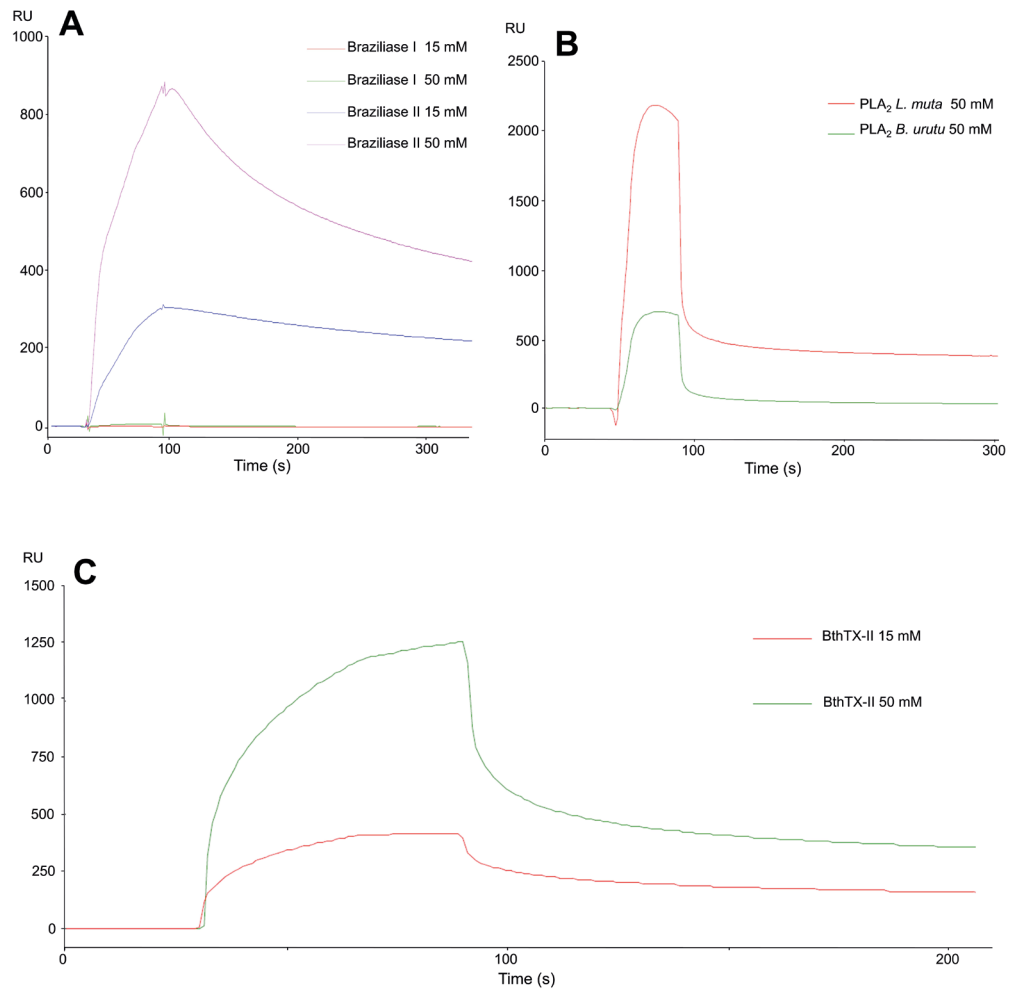


Figure 3. Binding assays between CatD and snake venom PLA₂s. **(A)** Interactions of CatD with Braziliase-I and Braziliase-II (concentrations of 15 and 50 μ M). **(B)** Responses were obtained from the interaction between CatD and svPLA₂s from *Bothrops neuwiedi urutu* (BnuTX-I) and *Lachesis muta* (LmutTX). **(C)** Interaction test between CatD and BthTX-II (concentrations of 15 and 50 mM). The analyzed samples were submitted to salt removal in a 5 mL Hitrap desalting (GE) column.

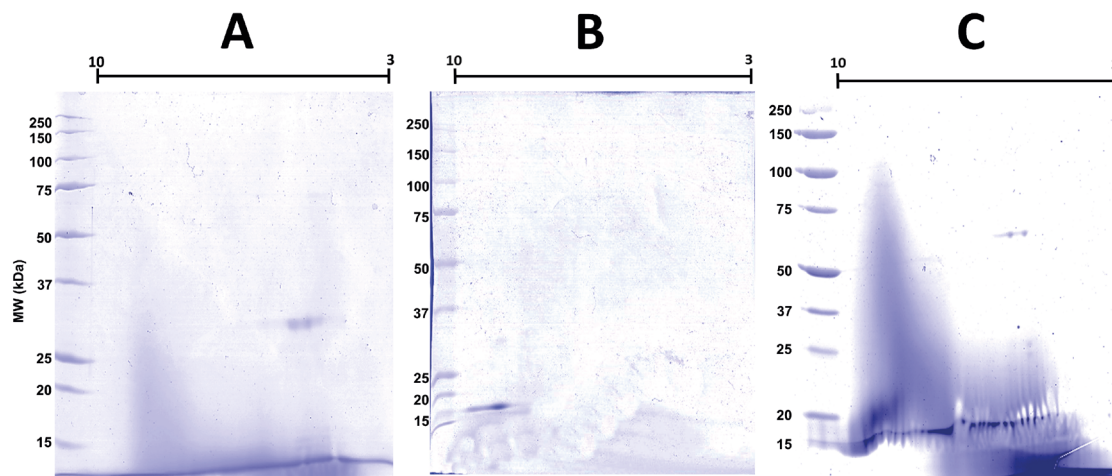


Figure 4. Two-dimensional SDS-PAGE: CatD, BthTX-II, and enzymatic complex. **(A)** Two-dimensional SDS-PAGE of CatD showing a pI of 4.74 and approximate molecular mass of 35 kDa. **(B)** Two-dimensional SDS-PAGE of BthTX-II with a pI of 8.74, with an approximate molecular mass of 14 kDa. **(C)** Two-dimensional SDS-PAGE of the complex with a pI of 5.79, and approximate molecular mass of 49 kDa.

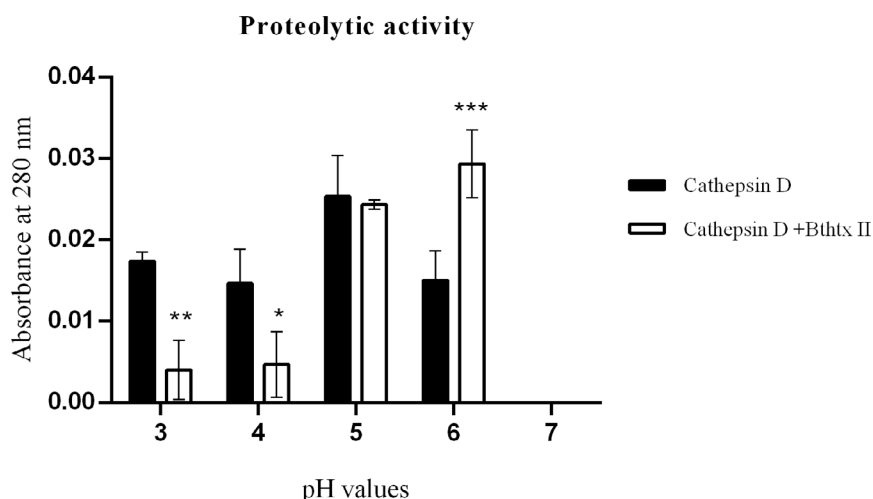


Figure 5. Proteolytic activity of CatD and the CatD + BthTX-II complex. The evaluation was performed at pHs 3, 4, 5, 6, and 7, identified in the figure legend, highlighting CatD in white (positive control) and the CatD + BthTX-II complex in black. As a negative control, the buffer itself (sodium citrate) was used at different pHs. The toxin used in the tests (BthTX-II) was submitted to contamination analysis (described in the second section). Two-way analysis of variance (ANOVA) with Tukey's multiple comparison post-test with significance level $p < 0.05$.

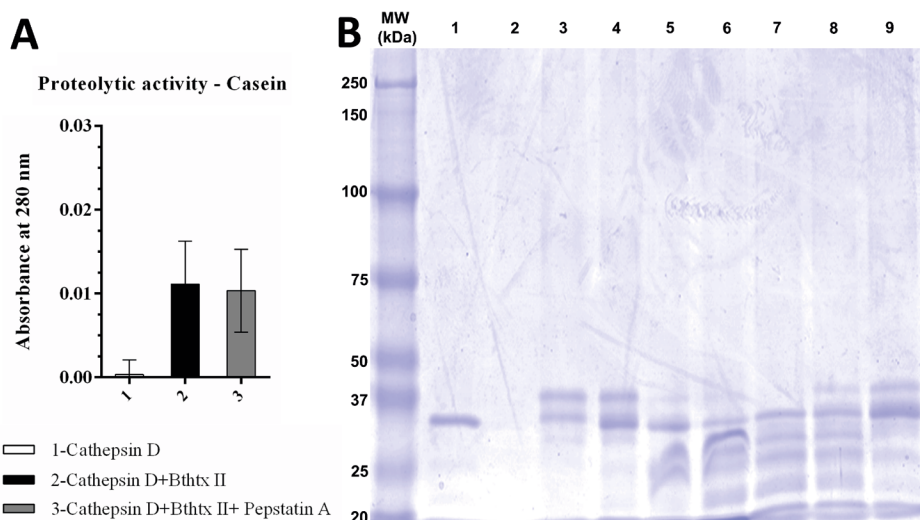


Figure 6. Proteolytic activity on casein. **(A)** Samples identified in the legend results: CatD, CatD + BthTX-II, CatD + BthTX-II + pepstatin A were considered negative controls; buffer (sodium citrate) was used at different pHs. **(B)** Proteolytic activities SDS-PAGE. Samples: (1) CatD; (2) pepstatin A (PepA); (3) casein; (4) CatD + PepA + casein; (5) CatD + casein; (6) CatD + BthTX-II Casein + PepA; (7) CatD + BthTX-II + casein (30 min); (8) CatD + BthTX-II + casein (15 min); (9) CatD + BthTX-II + casein (5 min). Samples 3 through 6 were incubated for 30 min at 27 °C. Positive control: CatD; negative control: pepstatin A (PepA).

Regarding the effects of the interaction of the CatD + BthTX-II complex on BthTX-II's catalytic function, the phospholipase activity assay (Fig. 7) shows that the complex's formation does not interfere with nor hinder BthTX-II's capability to cleave the artificial substrate 4N30BA. Interestingly, the presence of Pepstatin A slightly diminishes the catalytic output of the CatD + BthTX-II complex.

Structural analysis and molecular interaction simulations

All svPLA₂s showing interaction with CatD in the SPR assay and enzymatic assays were selected for further *in silico*

investigation, seeking details about the mechanism coordinating these interactions at the atomic level and the existence of common recognition sites for svPLA₂s on CatD's surface. Thus, five molecular docking methodologies were applied, effectively employing a consensus approach, which generated sets of docking conformations (Fig. 8) for each of the svPLAs₂ (BthTX-II, Braziliase-II and LmutTX). Additionally, the CatD + BthTX-II complex (Fig. 9) was subjected to a more intensive inspection due to its enzymatic activity. Molecular dynamics (MD) was used to evaluate the structural stability of this macromolecular assembly. Five independent replicas were simulated for 100 ns each. The processing and analysis of the generated trajectories

included an assessment of the CatD + BthTX-II complex's behavior in solution considering the radius of gyration (Fig. 10A) and RMSD (Fig. 10B) variations during the simulations. There were few noticeable fluctuations in the complex's backbone and its compactness. Nevertheless, the assembly formed between these two proteins remained stable through all five replicas. The interaction between CatD and BthTX-II was evaluated, using as

reference the central structures from the three most populated clusters generated in the clusterization performed with the sum of all five trajectories, exhibiting in that way an approximation of the most predominant conformation assumed by the CatD + BthTX-II complex during 500 ns of simulation (Fig. 10C). The absence of any remarkable shift in the complex's shape suggests an overall stable and cohesive interaction.

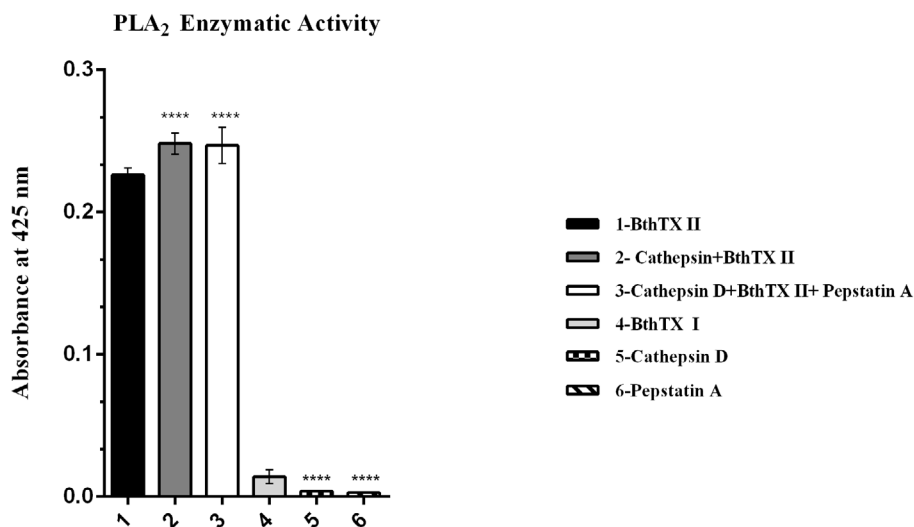


Figure 7. PLA₂ enzymatic activity on artificial substrate 4N3OBA. Samples: (1) BthTX-II; (2) CatD + BthTX-II; (3) CatD + BthTX-II + PepA; (4) BthTX-I; (5) CatD; (6) PepA. Positive control: BthTX-II. Negative control: BthTX-I.

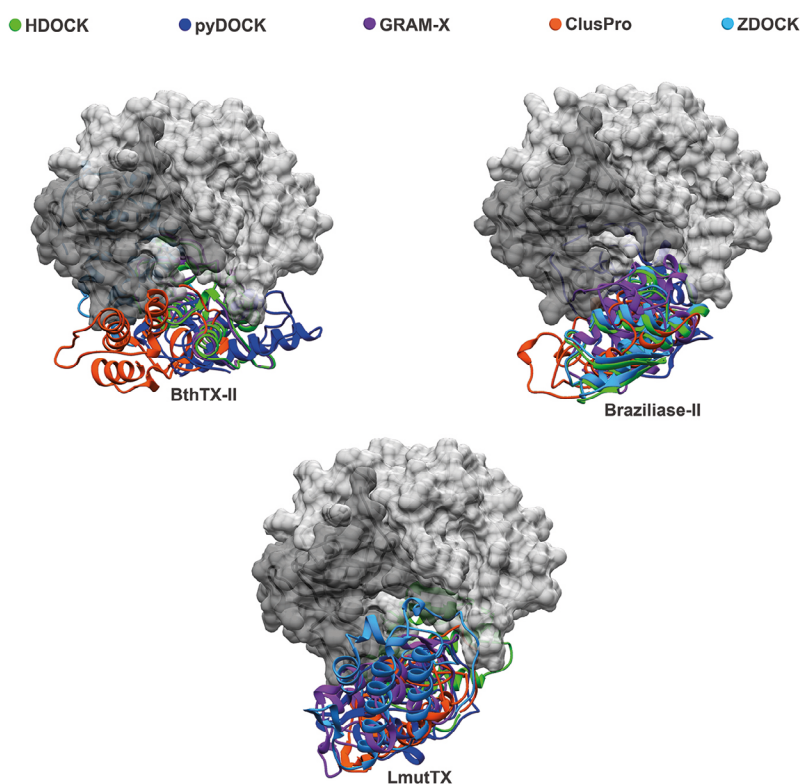


Figure 8. Molecular modeling of the interaction between three snake venom PLA₂s (LmuTX, Braziliase-II and BthTX-II) and human CatD using different docking tools (HDOCK, pyDOCK, GRAM-X, ClusPro, and ZDOCK). The CatD surface is represented in dark gray (light chain) and light gray (heavy chain). The svPLA₂s are colored according to the docking tool used.

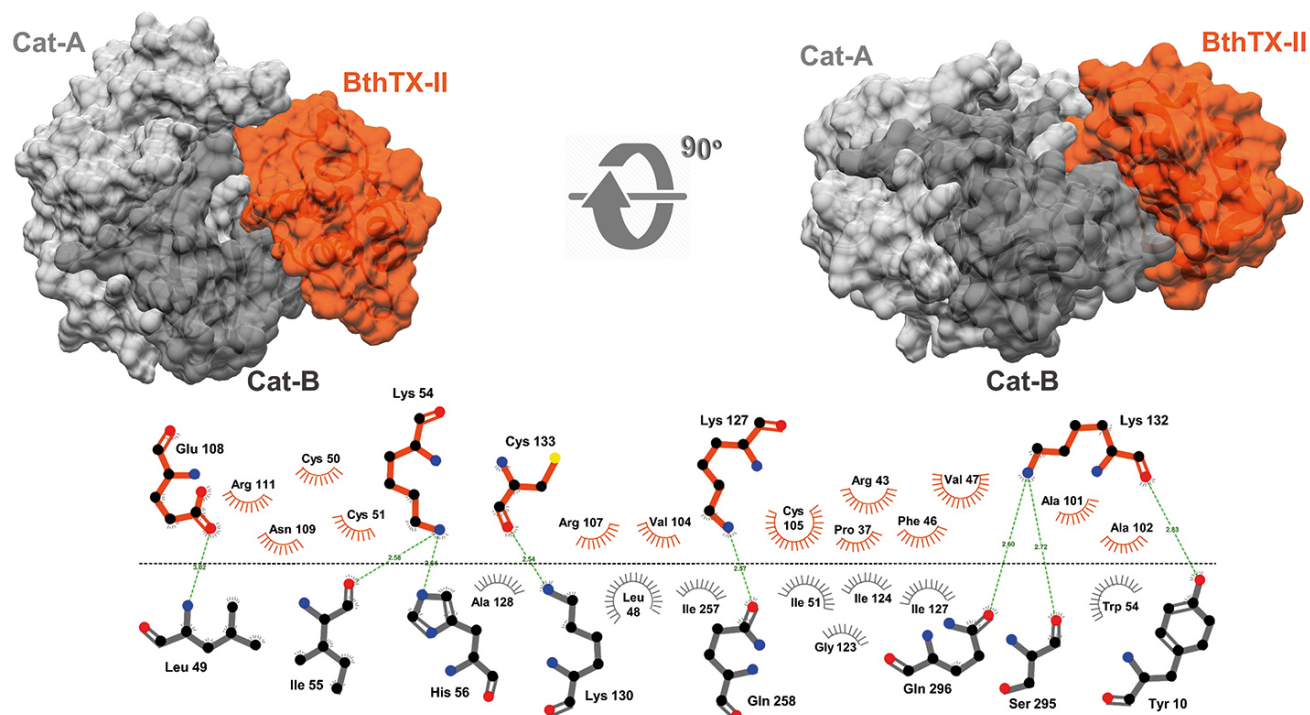


Figure 9. Molecular modeling of the CatD + BthTX-II complex. The complex formed between human CatD is shown in gray (light chain in dark gray and heavy chain in light gray) and BthTX-II is shown in orange. The interactions were enlarged to show amino acid residues in the interface and their interactions. H-bonds are highlighted by green dashed lines, and hydrophobic interactions are depicted as protrusions colored to match each amino acid residue.

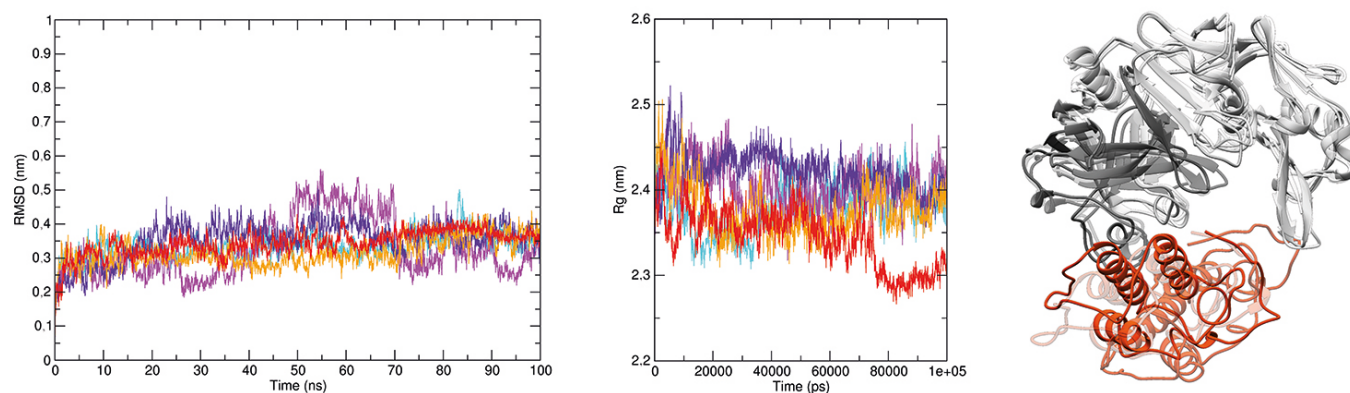


Figure 10. CatD + BthTX-II complex molecular dynamics. CatD is shown in gray (light chain in dark gray and heavy chain in light gray) and BthTX-II is shown in orange. The radius of gyration and backbone RMSD graphics are located on the left side of the figure. All five replicas are plotted in an overlapped manner in order to highlight all minor variations and overall stability throughout the 100 ns of each replica. The structures on the right end of the figure show a superposition respective to each of the three CatD + BthTX-II complexes representing the most predominant conformations during the total 500 ns simulated. These superposed complexes are the central structures extracted from the three most populated clusters generated in the clusterization analysis performed with the trajectories of all five replicas.

Discussion

In order to proceed with the characterization of the CatD + BthTX-II complex, different methodologies were used, such as Surface Plasmon Resonance (SPR), a detection method capable of performing real-time, label-free, and high-sensitivity monitoring of molecular interactions [64], and molecular docking, a key tool in structural molecular biology and computer-aided drug design, useful to predict structural data about a potential

protein-protein interaction using known three-dimensional structures [65].

SPR assays carried out with immobilized human CatD showed different levels of interaction with components of all snake venoms tested, ranging from 34.1 RU mg/mL for *C. d. cascavella* to 2,258.3 RU mg/mL for *B. jararacussu* (Table 1). The interaction of venom components with human cathepsin D, especially those from bothropic venoms, strongly suggests

that this could be an important and relevant new biological mechanism involving the participation of CatD and svPLA₂ in snake envenomation and other physiopathological processes with the participation of homologous proteins.

The use of *B. jararaca* venom cation exchange chromatographic fractions for further SPR assays (Fig. 2) showed that immobilized CatD interacted only with the last fractions (10, 11, and 12), which corresponds to well-known svPLA₂s, according to the monophoretic bands observed in the electrophoresis profile. This data indicated that the svPLA₂s presented in the samples tested in SPR binding assays with CatD could be the respective ligands. The SPR analyses carried out with the isolated svPLA₂s BthTX-II, Braziliase-II, BnuTX-I, and LmutTX revealed their ability to bind with immobilized human CatD (Fig. 3).

Two-dimensional electrophoresis showed that human CatD and BthTX-II form a stable complex of approximately 60 kDa and pI of 5.79. Initially, the apparent molecular mass and isoelectric point (pI) of the CatD + BthTX-II complex, as well as that of both enzymes separately, BthTX-II and CatD, were verified through two-dimensional electrophoresis (Fig. 4), determining a molecular mass for the CatD + BthTX-II complex. Next, the proteolytic activity of CatD and its complex with svPLA₂ (BthTX-II) was evaluated using casein as a substrate at pH values from 3 to 7, and Pepstatin A as a specific inhibitor. The pH optimum of the CatD + BthTX-II complex was found to be 6, while isolated CatD shows optimal activity at pH 4 [66]. Furthermore, Pepstatin A doesn't affect the CatD + BthTX-II complex activity with the substrate (Casein) at different pH values.

Interestingly, the change in CatD pH-dependent activity, when compared to that of the CatD + BthTX-II complex, is consistent with previous CatD studies in tumoral cell lines [67], suggesting that in the physiologic scenario, CatD's interaction with proteins such as svPLA₂ might be the factor allowing it to function in different pH ranges. Additionally, the CatD + BthTX-II complex was not inhibited by Pepstatin A, with CatD's catalytic activity remaining steady, further corroborating the CatD + BthTX-II complex's increased activity capacity. Moreover, the investigation of the CatD + BthTX-II complex's impact on BthTX-II's phospholipase activity suggests that the orientation of BthTX-II when coupled with CatD is ideal and allows BthTX-II to remain fully functional.

Computational simulations revealed a clear pattern of interaction between CatD and svPLA₂s, in such a way that all svPLA₂s tested in this study exhibited affinity by the concave surface formed between the heavy and light chain of CatD. This interaction profile was observed in every docking performed in this study. Furthermore, MD simulations done with the CatD + BthTX-II complex demonstrated that this may be the stable conformation assumed by CatD interacting with svPLA₂s in solution. Alone, the CatD + svPLA₂ complex's interface of interaction observed in the simulations performed herein is not able to enlighten the molecular mechanisms behind the boost in CatD's catalytic activity observed in the enzymatic assays. However, the conformation of the CatD + BthTX-II complex

generated in the docking predictions and later validated in the 500 ns of simulations agrees with the phospholipase activity assays. The capability of the CatD + BthTX-II complex to retain svPLA₂ makes perfect sense given BthTX-II's orientation upon attachment to CatD (Fig. 9 and 10C), in such a way that BthTX-II's hydrophobic channel and active site remain fully exposed to solvent.

Taking into account all these data, the *in silico* exploration of CatD's complex with svPLA₂ provides a clear basis for these two enzymes' interaction in the physiologic scenario. Nevertheless, it is necessary to carry out more experimental structural studies in order to confirm the modes of interaction between these enzymes. These results also raise new questions in the investigation of pathological and inflammatory symptoms of snake envenomation, in which CatD's interaction with svPLA₂ and the complexes formed could play an important role in the cascade of systemic and local effects present in snakebite accidents.

The interaction between CatD and svPLA₂ demonstrated herein will possibly have future implications for snakebite therapeutics. However, the most significant results extracted from this study may foreshadow more fundamental physiological issues involving the role of CatD in inflammatory processes, apoptosis and tumor progression. In this regard, the proteolytic process in neurons, in which CatD actively participates, is an essential maintenance step for the clearance of protein aggregates that reach the lysosomes through endocytosis and autophagy [24].

Di Domenico and coworkers proposed that the lack of control in protein repair (proteasome and lysosomal system) is a characteristic of degenerating neurons in Alzheimer's disease (AD), which highlights CatD's involvement in these conditions due to its essential role in the management of lysosomal integrity [33]. Thus, the rise in PLA₂ (IIA) in the cerebrospinal fluid of patients with AD indicates these enzymes as potential biomarkers in neuroinflammation [68, 69]. Furthermore, human brains affected by AD present a significant increase in PLA₂ mRNA in the hippocampus [70]. Interestingly, reports of PLA₂'s involvement in the destabilization of lysosomal membranes have been made in different experimental systems [29, 71, 72].

Overall, many approaches have discussed the involvement of PLA₂s in inflammatory processes [73–75]. In addition, PLA₂s also act on cell membrane metabolism and the production of arachidonic acid, a known precursor of prostaglandins, leukotrienes, and thromboxanes [76–78]. Johansson and coworkers demonstrated that incubation of PLA₂s with rat liver lysosomes resulted in the extravasation of its lysosomal constituents [29]. Additionally, Beaujouin and coworkers demonstrated CatD's involvement in apoptosis and showed that cancer cells that were pretreated with Pepstatin A, could not halt CatD nor hinder apoptosis, supporting the results described herein in the proteolytic activity assays. Moreover, CatD's capability to induce cancer cell growth, even when mutated, suggests an alternative mechanism for this enzyme [79].

Conclusion

For the first time, this study describes the formation of a functional multi-enzymatic complex between the human protease cathepsin D and snake venom phospholipases A₂. Collectively, the *in vitro* assays and *in silico* predictions carried out in this study demonstrated interaction and the formation of a new multi-enzymatic and catalytically active complex between CatD and svPLA₂. Additionally, the agreement between the data from previous studies regarding the pathways in which these enzymes are involved and the new data presented herein indicates the possibility of PLA₂ and CatD acting in conjunction in the extracellular environment [41]. Nevertheless, in the face of the many possible outcomes of this new enzymatic complex, the conclusions drawn must be taken with caution and, most importantly, warrant more extensive investigation on the subject.

Acknowledgments

The authors thank the Program for Technological Development in Tools for Health-PDTIS-FIOCRUZ for the use of its facilities.

Availability of data and materials

All data generated or analyzed during this study are included in this article.

Funding

The present study was supported by the Coordination for the Improvement of Higher Education Personnel (CAPES), National Council for Scientific and Technological Development (CNPq), Foundation for Support to the Development of Scientific and Technological Actions and the Rondônia Research (FAPERO), PDTIS/FIOCRUZ platforms, Center for the Study of Biomolecules Applied to Health-CEBio/FIOCRUZ-RO and Research Excellence Program (PROEP-FIOCRUZ), Fiocruz Rondônia.

Competing interests

The authors declare that they have no competing interests.

Authors' contributions

JNM, AMS and LAC conceived this research and designed experiments. JNM, LAC and AFF participated in the design and interpretation of data. JNM, AFF, LSMD, RDS, CS, TMRS, EAC and FBZ performed experiments and analysis. CASC, ACN, FBZ and MRMF wrote the paper and participated in the revisions of it. All authors read and approved the final manuscript.

Ethics approval

All snake venoms used in this study were acquired from the Venom Bank at CEBio/Fiocruz Rondônia/UNIR (Center for the Study of Biomolecules Applied to Health), Porto Velho, RO, Brazil, under local government authorization license number: IBAMA nº 27131-3 and CGEN/CNPq 010627/2011-1

Consent for publication

Not applicable.

References

1. Yadati T, Houben T, Bitorina A, Shiri-Sverdlov R. The ins and outs of cathepsins: Physiological function and role in disease management. *Cells*. 2020 Jul 13;9(7):1679. doi: [10.3390/cells9071679](https://doi.org/10.3390/cells9071679).
2. Turk V, Stoka V, Vasiljeva O, Renko M, Sun T, Turk B, Turk D. Cysteine cathepsins: From structure, function and regulation to new frontiers. *Biochim Biophys Acta*. 2012 Jan;1824(1):68–88. doi: [10.1016/j.bbapap.2011.10.002](https://doi.org/10.1016/j.bbapap.2011.10.002)
3. Patel S, Homaei A, El-Seedi HR, Akhtar N. Cathepsins: Proteases that are vital for survival but can also be fatal. *Biomed Pharmacother*. 2018 Sep;105:526–32. doi: [10.1016/j.biopha.2018.05.148](https://doi.org/10.1016/j.biopha.2018.05.148).
4. Brix K, Dunkhorst A, Mayer K, Jordans S. Cysteine cathepsins: cellular roadmap to different functions. *Biochimie*. 2008 Feb;90(2):194–207. doi: [10.1016/j.biochi.2007.07.024](https://doi.org/10.1016/j.biochi.2007.07.024).
5. Ward C, Martinez-Lopez N, Otten EG, Carroll B, Maetzel D, Singh R, Sarkar S, Korolchuk VI. Autophagy, lipophagy and lysosomal lipid storage disorders. *Biochim Biophys Acta*. 2016 Apr;1861(4):269–84. doi: [10.1016/j.bbali.2016.01.006](https://doi.org/10.1016/j.bbali.2016.01.006).
6. Stoka V, Turk V, Turk B. Lysosomal cathepsins and their regulation in aging and neurodegeneration. *Ageing Res Rev*. 2016 Dec;32:22–37. doi: [10.1016/j.arr.2016.04.010](https://doi.org/10.1016/j.arr.2016.04.010).
7. Bonnans C, Chou J, Werb Z. Remodelling the extracellular matrix in development and disease. *Nat Rev Mol Cell Biol*. 2014 Dec;15(12):786–801. doi: [10.1016/j.arr.2016.04.010](https://doi.org/10.1016/j.arr.2016.04.010).
8. Rakash S. Role of proteases in cancer: A review. *Biotechnol Mol Biol Rev*. 2012 Oct;7(4):90–101. doi: [10.5897/BMBR11.027](https://doi.org/10.5897/BMBR11.027).
9. Turk B, Turk V. Lysosomes as “Suicide Bags” in Cell Death: Myth or Reality? *J Biol Chem*. 2009 Aug 14;284(33):21783–7. doi: [10.1074/jbc.R109.023820](https://doi.org/10.1074/jbc.R109.023820).
10. Repnik U, Cesen MH, Turk B, Česen MH, Turk B. The endolysosomal system in cell death and survival. *Cold Spring Harb Perspect Biol*. 2013 Jan 1;5(1):a008755. doi: [10.1101/cshperspect.a008755](https://doi.org/10.1101/cshperspect.a008755).
11. Liaudet-Coopman E, Beaujouis M, Derocq D, Garcia M, Glondu-Lassis M, Laurent-Matha V, Prébois C, Rochefort H, Vignon F. Cathepsin D: newly discovered functions of a long-standing aspartic protease in cancer and apoptosis. *Cancer Lett*. 2006 Jun 18;237(2):167–79. doi: [10.1016/j.canlet.2005.06.007](https://doi.org/10.1016/j.canlet.2005.06.007).
12. Conus S, Perozzo R, Reinheckel T, Peters C, Scapozza L, Yousefi S, Simon HU. Caspase-8 is activated by cathepsin D initiating neutrophil apoptosis during the resolution of inflammation. *J Exp Med*. 2008 Mar 17;205(3):685–98. doi: [10.1074/jbc.M111.306399](https://doi.org/10.1074/jbc.M111.306399).
13. Mattson MP. Neuronal Life-and-Death Signaling, Apoptosis, and Neurodegenerative Disorders. *Antioxid Redox Signal*. 2006 Nov-Dec;8(11):1997–2006. doi: [10.1038/35040009](https://doi.org/10.1038/35040009).
14. Sato Y, Suzuki Y, Ito E, Shimazaki S, Ishida M, Yamamoto T, Yamamoto H, Toda T, Suzuki M, Suzuki A, Endo T. Identification and characterization of an increased glycoprotein in aging: Age-associated translocation of cathepsin D. *Mech Ageing Dev*. 2006;127:771–8. doi: [10.1016/j.mad.2006.07.001](https://doi.org/10.1016/j.mad.2006.07.001).
15. Garcia M, Platet N, Liaudet E, Laurent V, Derocq D, Brouillet J, Rochefort H. Biological and clinical significance of cathepsin D in breast cancer metastasis. *Stem Cells*. 1996 Nov;14(6):642–50. doi: [10.1002/stem.140642](https://doi.org/10.1002/stem.140642).
16. Metcalf P, Fusek M. Two crystal structures for cathepsin D: the lysosomal targeting signal and active site. *EMBO J*. 1993 Apr;12(4):1293–302. doi: [10.1002/j.1460-2075.1993.tb05774.x](https://doi.org/10.1002/j.1460-2075.1993.tb05774.x).
17. Baldwin ET, Bhat TN, Gulnik S, Hosur M V., Sowder RC, Cachau RE, Collins J, Silva AM, Erickson JW. Crystal structures of native and inhibited forms of human cathepsin D: implications for lysosomal targeting and drug design. *Proc Natl Acad Sci U S A*. 1993 Jul 15;90(14):6796–800. doi: [10.1073/pnas.90.14.6796](https://doi.org/10.1073/pnas.90.14.6796).
18. Zaidi N, Maurer A, Niek S, Kalbacher H. Cathepsin D: A cellular roadmap. *Biochem Biophys Res Commun*. 2008 Nov 7;376(1):5–9. doi: [10.1016/j.bbrc.2008.08.099](https://doi.org/10.1016/j.bbrc.2008.08.099).

19. Benes P, Vetvicka V, Fusek M. Cathepsin D - Many functions of one aspartic protease. *Crit Rev Oncol Hematol*. 2008 Oct;68(1):12–28. doi: 10.1016/j.critrevonc.2008.02.008.
20. Masson O, Bach AS, Deroocq D, Prébois C, Laurent-Matha V, Patingre S, Liaudet-Coopman E. Pathophysiological functions of cathepsin D: Targeting its catalytic activity versus its protein binding activity? *Biochimie*. 2010;92:1635–43. doi: 10.1016/j.biochi.2010.05.009.
21. Chaudhary H, Jena KP, Trivedi D, Purabdhari K, Vora N, Nair P, Sangtani K, Thakur S, Saini A, Singh S, Patel JSS. Cathepsin D: A novel target for apoptotic induction, as a future anti-cancer therapy: a review. *J Phys Pharm Adv J Phys Pharm Adv*. 2012 Feb 1;2(2):87–96.
22. Khalkhali-Ellis Z, Hendrix MJC. Two faces of cathepsin D: Physiological guardian angel and pathological demon. *Biol Med (Aligarh)*. 2014 Jul;6(2):1000206. doi: 10.4172/0974-8369.1000206.
23. Gocheva V, Joyce JA. Cysteine cathepsins and the cutting edge of cancer invasion. *Cell Cycle*. 2007 Jan 1;6(1):60–4. doi: 10.4161/cc.6.1.3669.
24. Fusek M, Vetvicka V. Dual role of cathepsin D: ligand and protease. *Biomed Pap Med Fac Univ Palacky Olomouc Czech Repub*. 2005 Jun;149(1):43–50. doi: 10.5507/pb.2005.003.
25. Johansson AC, Steen H, Öllinger K, Roberg K. Cathepsin D mediates cytochrome c release and caspase activation in human fibroblast apoptosis induced by staurosporine. *Cell Death Differ*. 2003 Nov;10(11):1253–9. doi: 10.1038/sj.cdd.4401290
26. Arnold D, Keilholz W, Schild H, Dumrese T, Stevanovic S, Rammensee HG. Substrate specificity of cathepsins D and E determined by N-terminal and C-terminal sequencing of peptide pools. *Eur J Biochem*. 1997 Oct 1;249(1):171–9. doi: 10.1111/j.1432-1033.1997.t01-1-00171.x.
27. Pimenta DC, Oliveira A, Juliano MA, Juliano L. Substrate specificity of human cathepsin D using internally quenched fluorescent peptides derived from reactive site loop of kallistatin. *Biochim Biophys Acta*. 2001 Jan 12;1544(1-2):113–22. doi: 10.1016/s0167-4838(00)00209-0.
28. Appelqvist H, Johansson A, Linderöth E, Johansson U, Antonsson B, Steinfeld R, Kagedal K, Öllinger K. Lysosome-mediated apoptosis is associated with cathepsin D-specific processing of bid at Phe24, Trp48, and Phe183. *Ann Clin Lab Sci*. 2012 Summer;42(3):231–42.
29. Charlotte Johansson A, Appelqvist AJH, Nilsson C, Kagedal K, Roberg K, Öllinger K. Regulation of apoptosis-associated lysosomal membrane permeabilization. *Apoptosis*. 2010 May;15(5):527–40. doi: 10.1007/s10495-009-0452-5
30. Castino R, Isidoro C, Murphy D. Autophagy-dependent cell survival and cell death in an autosomal dominant familial neurohypophyseal diabetes insipidus *in vitro* model. *FASEB J*. 2005 Jun;19(8):1024–6. doi: 10.1096/fj.04-3163fje.
31. Saftig P, Hetman M, Schmahl W, Weber K, Heine L, Mossmann H, Koster A, Hess B, Evers M, von Figura K. Mice deficient for the lysosomal proteinase cathepsin D exhibit progressive atrophy of the intestinal mucosa and profound destruction of lymphoid cells. *EMBO J*. 1995 Aug 1;14(15):3599–608. doi: 10.1002/j.1460-2075.1995.tb00029.x.
32. Crabtree D, Dodson M, Ouyang X, Boyer-Guittaut M, Liang Q, Ballestas ME, Fineberg N, Zhang J. Over-expression of an inactive mutant cathepsin D increases endogenous alpha-synuclein and cathepsin B activity in SH-SY5Y cells. *J Neurochem*. 2014 Mar;128(6):950–61. doi: 10.1111/jnc.12497.
33. Di Domenico F, Tramutola A, Perluigi M. Cathepsin D as a therapeutic target in Alzheimer's disease. *Expert Opin Ther Targets*. 2016 Dec;20(12):1393–5. doi: 10.1080/14728222.2016.1252334.
34. Zhao CF, Herrington DM. The function of cathepsins B, D, and X in atherosclerosis. *Am J Cardiovasc Dis*. 2016;6(4):163–70.
35. Olson OC, Joyce JA. Cysteine cathepsin proteases: regulators of cancer progression and therapeutic response. *Nat Rev Cancer*. 2015 Dec;15(12):712–29. doi: 10.1038/nrc4027.
36. Palermo C, Joyce JA. Cysteine cathepsin proteases as pharmacological targets in cancer. *Trends Pharmacol Sci*. 2008 Jan;29(1):22–8. doi: 10.1016/j.tips.2007.10.011.
37. Almeida JR, Resende LM, Watanabe RK, Carregari VC, Huancahuire-Vega S, da S. Caldeira CA, Coutinho-Neto A, Soares AM, Vale N, Gomes PAC, Marangoni S, Calderon LA, Silva SL. Snake venom peptides and low mass proteins: Molecular tools and therapeutic agents. *Curr Med Chem*. 2017;24(30):3254–82. doi: 10.2174/0929867323666161028155611.
38. Silva GM da, Souza DHB de, Waitman KB, Ebram MC, Fessel MR, Zainescu IC, Portaro FC, Heras M, Andrade SA. Design, synthesis, and evaluation of *Bothrops* venom serine protease peptidic inhibitors. *J Venom Anim Toxins incl Trop Dis*. 2021;27. doi: 10.1590/1678-9199-JVATITD-2020-0066.
39. Murakami M, Taketomi Y, Girard C, Yamamoto K, Lambeau G. Emerging roles of secreted phospholipase A2 enzymes: Lessons from transgenic and knockout mice. *Biochimie*. 2010 Jun;92(6):561–82. doi: 10.1016/j.biochi.2010.03.015.
40. Fortes-Dias CL, Macedo DHF, Barbosa RP, Souza-Silva G, Ortolani PL. Identification and characterization of the first endogenous phospholipase A₂ inhibitor from a non-venomous tropical snake, *Boa constrictor* (Serpentes: Boidae). *J Venom Anim Toxins incl Trop Dis*. 2020;26. doi: 10.1590/1678-9199-JVATITD-2019-0044.
41. Burke JE, Dennis EA. Phospholipase A₂ structure/function, mechanism, and signaling. *J Lipid Res*. 2009 Apr;50(Suppl):S237–42. doi: 10.1194/jlr.R800033-JLR200.
42. Gutiérrez JM, Lomonte B. Phospholipases A₂: Unveiling the secrets of a functionally versatile group of snake venom toxins. *Toxicon*. 2013 Feb;62:27–39. doi: 10.1016/j.toxicon.2012.09.006.
43. Xiong S, Huang C. Synergistic strategies of predominant toxins in snake venoms. *Toxicol Lett*. 2018 May 1;287:142–54. doi: 10.1016/j.toxlet.2018.02.004.
44. Péterfi O, Boda F, Szabó Z, Ferencz E, Bába L. Hypotensive snake venom components -A Mini-review. *Molecules*. 2019 Jul 31;24(15):2778. doi: 10.3390/molecules24152778.
45. Harris J, Scott-Davey T. Secreted phospholipases A₂ of snake venoms: Effects on the peripheral neuromuscular system with comments on the role of phospholipases A₂ in disorders of the CNS and their uses in industry. *Toxins (Basel)*. 2013 Dec 17;5(12):2533–71. doi: 10.3390/toxins5122533.
46. Diniz-Sousa R, Caldeira CAS, Kayano AM, Paloschi M V, Pimenta DC, Simões-Silva R, Ferreira AS, Zanchi FB, Matos NB, Grabner FP, Calderon LA, Zuliani JP, Soares AM. Identification of the molecular determinants of the antibacterial activity of LmutTX, a Lys49 phospholipase A₂ homologue isolated from *Lachesis muta muta* snake venom (Linnaeus, 1766). *Basic Clin Pharmacol Toxicol*. 2018 Apr;122(4):413–23. doi: 10.1111/bcpt.12921.
47. Correa EA, Kayano AM, Diniz-Sousa R, Setubal SS, Zanchi FB, Zuliani JP, Matos NB, Almeida JR, Resende LM, Marangoni S, Silva SL, Soares AM, Calderon LA. Isolation, structural and functional characterization of a new Lys49 phospholipase A₂ homologue from *Bothrops neuwiedi urutu* with bactericidal potential. *Toxicon*. 2016 Jun 1;115:13–21. doi: 10.1016/j.toxicon.2016.02.021.
48. Kayano AM, Simões-Silva R, Medeiros PSM, Maltarollo VG, Honorio KM, Oliveira E, Albericio F, Silv SI, Aguiar ACC, Krettl AU, Fernandes CFC, Juliani JP, Calderon LA, Stábeli RG, Soares AM. BbMP-1, a new metalloproteinase isolated from *Bothrops brazili* snake venom with *in vitro* antiparasitoid properties. *Toxicon*. 2015 Nov;106:30–41. doi: 10.1016/j.toxicon.2015.09.005.
49. Sobrinho JC, Kayano AM, Simões-Silva R, Alfonso JJ, Gomez AF, Gomez MCV, Zanchi FB, Moura LA, Souza VR, Fuly AL, Oliveira E, Silva SL, Almeida JR, Zuliani JP, Soares AM. Anti-platelet aggregation activity of two novel acidic Asp49-phospholipases A₂ from *Bothrops brazili* snake venom. *Int J Biol Macromol*. 2018 Feb;107(Pt A):1014–22. doi: 10.1016/j.ijbiomac.2017.09.069.
50. Bradford MM. A rapid and sensitive method for the quantitation of microgram quantities of protein utilizing the principle of protein-dye binding. *Anal Biochem*. 1976 May 7;72:248–54. doi: 10.1006/abio.1976.9999.
51. Rodrigues VM, Soares AM, Guerra-Sá R, Rodrigues V, Fontes MRM, Giglio JR. Structural and functional characterization of newwiedase, a nonhemorrhagic fibrin(ogen)olytic metalloprotease from *Bothrops neuwiedi* snake venom. *Arch Biochem Biophys*. 2000 Sep 15;381:213–24. doi: 10.1006/abbi.2000.1958.
52. Petrovic N, Grove C, Langton PE, Misso NLA, Thompson PJ. A simple assay for a human serum phospholipase A2 that is associated with high-density lipoproteins. *J Lipid Res*. 2001 Oct;42(10):1706–13. doi: 10.1016/S0022-2275(20)32226-4

53. Song Y, DiMaio F, Wang RYR, Kim D, Miles C, Brunette T, Thompson J, Baker D. High resolution comparative modeling with RosettaCM. Structure. 2013 Oct 8;21(10):1735-42. doi: 10.1016/j.str.2013.08.005.
54. Huang J, Rauscher S, Nawrocki G, Ran T, Feig M, De Groot BL, et al. CHARMM36m: An improved force field for folded and intrinsically disordered proteins. Nat Methods. 2016 Nov 7;14:71-3. doi: 10.1038/nmeth.4067.
55. Bussi G, Donadio D, Parrinello M. Canonical sampling through velocity rescaling. J Chem Phys. 2007 Jan 7;126(1):014101. doi: 10.1063/1.2408420.
56. Berendsen HJC, Postma JPM, Van Gunsteren WF, Dinola A, Haak JR. Molecular dynamics with coupling to an external bath. J Chem Phys. 1984 Jun 27;81(1984):3684-90. doi: 10.1063/1.448118.
57. Hoover WG. Canonical dynamics: Equilibrium phase-space distributions. Phys Rev A. 1985 Mar;31(3):1695-7. doi: 10.1103/PhysRevA.31.1695.
58. Parrinello M, Rahman A. Polymorphic transitions in single crystals: A new molecular dynamics method. J Appl Phys. 1981;52:7182-90. doi: 10.1063/1.328693.
59. Daura X, Gademann K, Jaun B, Seebach D, van Gunsteren WF, Mark AE. Peptide folding: When simulation meets experiment. Angew Chemie Int Ed. 1999;38(1-2):236-40. doi: 10.1002/(SICI)1521-3773(19990115)38:1/2%3C236::AID-ANIE236%3E3.0.CO;2-M.
60. Petterson EF, Goddard TD, Huang CC, Couch GS, Greenblatt DM, Meng EC, Ferrin TE. UCSF Chimera - A visualization system for exploratory research and analysis. J Comput Chem. 2004 Oct;25(13):1605-12. doi: 10.1002/jcc.20084.
61. Andrião-Escarso SH, Soares AM, Rodrigues VM, Angulo Y, Díaz C, Lomonte B, Gutiérrez JM, Giglio JR. Myotoxic phospholipases A₂ in *Bothrops* snake venoms: Effect of chemical modifications on the enzymatic and pharmacological properties of bothropstoxins from *Bothrops jararacussu*. Biochimie. 2000 Aug;82(8):755-63. doi: 10.1016/s0300-9084(00)01150-0.
62. Dennis EA, Cao J, Hsu YH, Magrioti V, Kokotos G. Phospholipase A₂ enzymes: Physical structure, biological function, disease implication, chemical inhibition, and therapeutic intervention. Chem Rev. 2011 Oct 12;111(10):6130-85. doi: 10.1021/cr200085w.
63. Conner GE. Cathepsin D. Handb proteolytic enzym. Barrett A, Rawlings N, Woessner J editors. Elsevier; 2004. p. 43-52. doi: 10.1016/B978-0-12-382219-2.00281-7.
64. Nguyen HH, Park J, Kang S, Kim M. Surface plasmon resonance: A versatile technique for biosensor applications. Sensors (Basel). 2015 May 5;15(5):10481-510. doi: 10.3390/s150510481.
65. Morris GM, Lim-Wilby M. Molecular docking. Methods Mol Biol. 2008;443:365-82. doi: 10.1007/978-1-59745-177-2_19.
66. Sapolsky AI, Howell DS, Woessner, JF Jr. Neutral proteases and cathepsin D in human articular cartilage. J Clin Invest. 1974 Apr;53(4):1044-53. doi: 10.1172/JCI107641.
67. Maynadier M, Farnoud R, Lamy P-J, Laurent-Matha V, Garcia M, Rochefort H. Cathepsin D stimulates the activities of secreted plasminogen activators in the breast cancer acidic environment. Int J Oncol. 2013 Nov;43(5):1683-90. doi: 10.3892/ijo.2013.2095.
68. Tasoulis T, Isbister GK. A review and database of snake venom proteomes. Toxins (Basel). 2017 Sep 18;9(9):290. doi: 10.3390/toxins9090290.
69. Turk V, Kos J, Turk B. Cysteine cathepsins (proteases) - On the main stage of cancer? Cancer Cell. 2004 May;5(5):409-10. doi: 10.1016/s1535-6108(04)00117-5.
70. Moses GS, Jensen MD, Lue L-F, Walker DG, Sun AY, Simonyi A, Sun GY. Secretory PLA₂-IIA: a new inflammatory factor for Alzheimer's disease. J Neuroinflammation. 2006 Oct 7;3:28. doi: 10.1186/1742-2094-3-28.
71. Mirnikjoo B, Balasubramanina K, Schroit AJ. Mobilization of lysosomal calcium regulates the externalization of phosphatidylserine during Apoptosis. J Biol Chem. 2009 Mar 13;284(11):6918-23. doi: 10.1074/jbc.M805288200.
72. Windelborn JA, Lipton P. Lysosomal release of cathepsins causes ischemic damage in the rat hippocampal slice and depends on NMDA-mediated calcium influx, arachidonic acid metabolism, and free radical production. J Neurochem. 2008 Jul;106(1):56-69. doi: 10.1111/j.1471-4159.2008.05349.x.
73. Murakami M, Taketomi Y, Miki Y, Sato H, Hirabayashi T, Yamamoto K. Progress in Lipid Research Recent progress in phospholipase A₂ research: from cells to animals to humans. Prog Lipid Res. 2011;50:152-92. doi: 10.1016/j.plipres.2010.12.001.
74. Murakami M, Sato H, Miki Y, Yamamoto K, Taketomi Y. A new era of secreted phospholipase A₂. J Lipid Res. 2015 Jul;56(7):1248-61. doi: 10.1194/jlr.R058123.
75. Murakami M, Yamamoto K, Miki Y, Murase R, Sato H, Taketomi Y. The roles of the secreted phospholipase A₂ gene family in immunology. Adv Immunol. 2016;132:91-134. doi: 10.1016/bs.ai.2016.05.001.
76. Ricciotti E, Fitzgerald GA. Prostaglandins and inflammation. Arterioscler Thromb Vasc Biol. 2011 May;31(5):986-1000. doi: 10.1161/ATVBAHA.110.207449.
77. Nicotra G, Castino R, Follo C, Peracchio C, Valente G, Isidoro C. The dilemma: Does tissue expression of cathepsin D reflect tumor malignancy? the question: Does the assay truly mirror cathepsin D mis-function in the tumor? Cancer Biomark. 2010 Oct;7(1):47-64. doi: 10.3233/CBM-2010-0143.
78. Oliveira CS, Caldeira CAS, Diniz-sousa R, Romero DL, Marcussi S, Moura LA, Fuly AL, de Carvalho C, Cavalcante WLG, Gallacci M, Dal Pai M, Zuliani JP, Calderon LA, Soares AM. Pharmacological characterization of cnidarian extracts from the Caribbean Sea: evaluation of anti-snake venom and antitumor properties. J Venom Anim Toxins incl Trop Dis. 2018;1-11. doi: 10.1186/s40409-018-0161-z.
79. Beaujouin M, Baghdiguan S, Glondu-Lassis M, Berchem G, Liaudet-Coopman E. Overexpression of both catalytically active and -inactive cathepsin D by cancer cells enhances apoptosis-dependent chemosensitivity. Oncogene. 2006;25:1967-73. doi: 10.3390/cells9071679.